

# Mechanical and Tribological Properties of DLC Films for Sliding Parts

Dr. Hirotaka ITO\*<sup>1</sup>, Dr. Kenji YAMAMOTO\*<sup>1</sup>

\*<sup>1</sup> Materials Research Lab., Technical Development Group

Diamond-like carbon (DLC) film has the advantage of having both low friction and low wear, and in recent years it has been applied to various sliding parts, such as parts for internal-combustion automotive engines. This paper presents a study on the mechanical characteristics and sliding properties of DLC films deposited by unbalanced magnetron sputtering (UBMS) equipment. It was clarified that the UBMS equipment can control the amount of hydrogen in a DLC film and as a consequence the mechanical properties of the DLC film can be changed. Furthermore, sliding tests using oil lubrication clarified that controlling the amount of hydrogen in DLC and the choice of additives in the oil are critical to achieving both low friction and low wear at the same time.

## Introduction

Diamond-like carbon (hereinafter referred to as DLC) films have been attracting attention as a material that achieves both low friction and low wear at the same time. In recent years, the films are being increasingly used in the automotive field with a view to saving energy. Their applications include automobile engine parts such as valve lifters,<sup>1)</sup> piston rings,<sup>2)</sup> injectors for diesel engine common rail systems<sup>3)</sup> and electromagnetic clutch plates.<sup>4)</sup> In cases where DLC is used in engine oil, issues of compatibility with the engine oil have been pointed out, along with the properties of the DLC film.<sup>1)</sup> In the future, DLC films are expected to be applied not only in the automotive field, but also in various other fields such as general mechanical parts and electronics.

Kobe Steel has a lineup of unbalanced magnetron sputtering (hereinafter referred to as "UBMS") apparatuses for depositing DLC films. This paper describes the structures and mechanical properties of DLC films deposited by a UBMS apparatus under various deposition conditions, as well as the sliding properties of the DLC films obtained.

DLC films are classified by ternary diagram based on hydrogen content and  $sp^2/sp^3$  bonding ratio (Fig. 1).<sup>5)</sup> The films containing no hydrogen are called hydrogen-free DLC films, or amorphous carbon ( $a-C$ ); those with a high ratio of  $sp^3$  bonding, which forms a tetrahedral structure, the crystal structure of diamond, are referred to as tetrahedral amorphous carbon ( $ta-C$ ). The films containing hydrogen are classified as hydrogenated amorphous

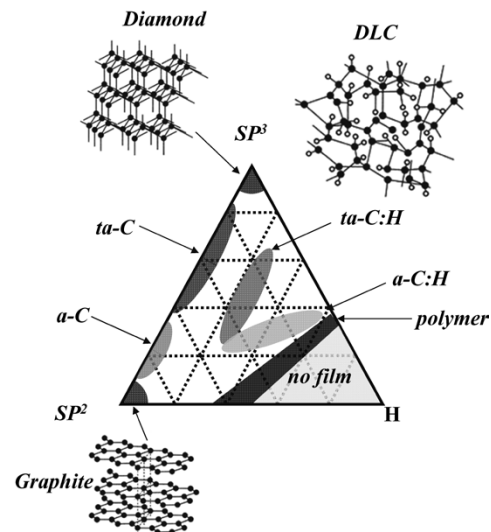


Fig. 1 Ternary diagram of DLC and schematic images of DLC structure

carbon ( $a-C:H$ ) and hydrogenated tetrahedral amorphous carbon ( $ta-C:H$ ). In many cases,  $a-C$ ,  $a-C:H$ ,  $ta-C$ , and  $ta-C:H$  are collectively referred to as DLC. The properties of the films can be controlled by introducing constituents other than hydrogen or carbon, and films containing various metals,<sup>6)</sup> Si<sup>4)</sup> and/or nitrogen<sup>7)</sup> are also referred to as DLC films in a broad sense; however, these films with elements other than carbon or hydrogen cannot be included in the classification shown in Fig. 1.

The UBMS process described in this paper can deposit DLC film mainly in the regions designated as  $a-C$  and  $a-C:H$  in Fig. 1. The following describes a study conducted on the advantage and sliding properties of DLC films that can be deposited by the UBMS process.

## 1. Test method

Assuming application to automobile engine parts, a sliding test in lubricating oil was conducted on DLC films deposited under various conditions of the UBMS process. This sliding test not only indicates the relationship between the deposition conditions of DLC films and their mechanical properties, but also enables the investigation of how the hydrogen content in DLC films, as well as the additives contained in the lubricating oil, influence the sliding properties.

## 1.1 Deposition method

A schematic diagram of an UBMS apparatus is shown in Fig. 2. The inner and outer magnets placed behind a target generate a magnetic field with asymmetric strength, the magnetic field extending to the substrate side, enlarging the plasma region. Application of bias voltage to the substrate during deposition ensures the implantation of argon (Ar) ions from the plasma near the substrate, enabling the control of film properties such as hardness and surface roughness. For the details of the UBMS process, reference may be made to published articles.<sup>9)</sup>

The film deposition described in this paper was accomplished using a compact UBMS apparatus (UBMS 202) manufactured by Kobe Steel. The targets used were carbon (C) and chromium (Cr) disks, each having a diameter of 6 inches. Formation of an intermediate layer is important to ensure adhesion between a substrate and DLC film, which is chemically inactive by nature. In the case of iron-based substrates, for example, the construction of Cr/WC/WC-C gradient composition/DLC film<sup>10)</sup> ensures the adhesion strength of the interfaces at both the substrate/intermediate layers and intermediate layer/DLC film to withstand the sliding in environments such as automobile engine parts. The experiments in this paper do not require a specific level of adhesion for actual parts and adopted a more convenient construction of Cr/WC/WC-C gradient composition/DLC film.

The DLC deposition was conducted in the apparatus with a substrate (a cemented carbide insert, a Si (100) wafer, or a SKH51 disk) installed. The chamber was evacuated to  $2 \times 10^{-3}$  Pa or below, which was followed by argon (Ar) ion bombardment for substrate surface cleaning before the deposition of the intermediate layer. The intermediate layer was formed by first depositing a Cr layer, followed by the deposition of a Cr-C gradient composition

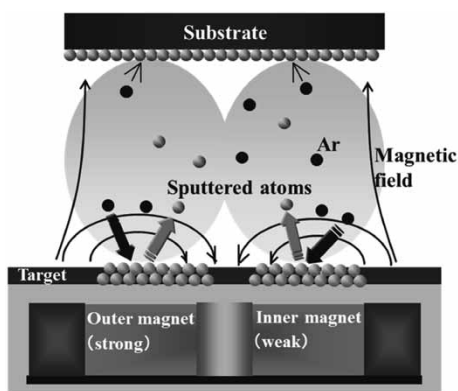


Fig. 2 Schematic image of UBMS<sup>8)</sup>

layer, during which the sputtering power and the amount of introduced gas (Ar and CH<sub>4</sub>) were controlled. After forming the intermediate layer of Cr/Cr-C gradient composition, a DLC layer was deposited under varying deposition conditions. During the DLC deposition, Ar and CH<sub>4</sub> gas were introduced and the total gas pressure was adjusted to 0.6 Pa. The hydrogen content in the DLC films was controlled by the flow rate ratio of the Ar and CH<sub>4</sub> gas introduced.

## 1.2 Evaluation method

The surface roughness of DLC films after deposition was measured with an atomic force microscope (hereinafter referred to as "AFM"). Hardness was measured using a nano-indenter based on the Berkovich diamond indenter, and the hardness values were calculated in accordance with the Sawa/Tanaka method<sup>11)</sup> with the correction for indenter tip. The structures of DLC films were analyzed by Raman spectrometry, the film density was measured using Rutherford backscattering spectrometry (hereinafter referred to as "RBS"), and the hydrogen content was analyzed by elastic recoil detection analysis (hereinafter referred to as ERDA).

The sliding test was carried out using a friction and wear tester (Tri-Bot) manufactured by Shinko Engineering Co., Ltd. Fig. 3 shows a schematic diagram of the sliding test. Various DLC films were deposited on SKH 51 disks ( $\phi$  55 mm  $\times$  5 mm). Two vane samples (ea. 3.5 mm  $\times$  5.0 mm  $\times$  14 mm; tip radius, 5 mm) made of high-carbon chromium bearing steel (SUJ2) were used.

In the sliding test, each disk was placed on a vane in lubricating oil, and the disk was rotated while a load was applied. For lubricating oil, poly- $\alpha$ -olefin (PAO), a synthetic hydrocarbon, was used as the base oil. As for additive agent, ester-type glycerin monooleate (GMO) was used; it is known to exhibit a low friction coefficient when combined with DLC

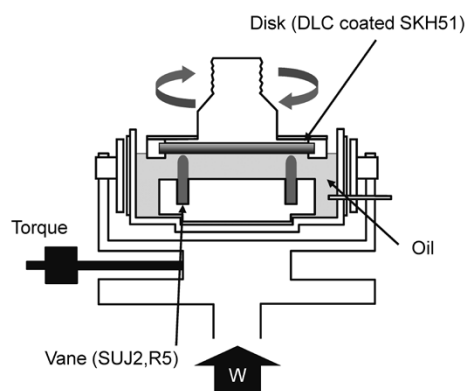


Fig. 3 Schematic image of sliding equipment

film containing no hydrogen.<sup>1)</sup> In addition, two types of lubricating oil respectively containing 3 wt% of phosphite and amine phosphate, both being phosphorus additive agents were also used with the remainder of the base oil. The testing conditions were: applied load of 500N, lubricating oil temperature at 80°C and sliding speed reduced step-by-step from 0.09m/s to 0.02m/s.

After the sliding test the samples were observed with an optical microscope. The wear volume was calculated by measuring the worn cross-sectional profile of each sliding part with a surface profiler. For more detailed analysis of sliding parts, the cross-sections of worn portions were observed by transmission electron microscopy (hereinafter referred to as "TEM"), while compositions were analyzed by Auger electron spectroscopy analysis (hereinafter referred to as "AES").

## 2. Test results and discussion

### 2.1 Change of DLC film properties due to deposition conditions

Controlling the bias voltage applied to substrates during DLC deposition to implant Ar has been expected to improve the quality of DLC films. Fig. 4 shows the change in DLC film hardness when it is deposited with varying bias voltage applied to the substrates. This figure shows that the hardness of DLC films increases with enhanced negative bias voltage; however, the hardness exhibits no change when the negative bias voltage is greater than 150V. Fig. 5 shows the results of AFM observation of the surface nanostructures of the DLC films deposited under different bias voltage conditions. The surface roughness (Ra) was Ra=3.9nm when the bias voltage was 0V and Ra=0.43nm at -200V. It was confirmed that the surface becomes smoother with the increasing negative bias voltage. Taking into consideration the fact that the deposition rate of DLC film decreases with enhanced bias voltage, along with the results above, enhancing the bias voltage of UBMS is considered to have caused the smoothing of the surface by Ar ion etching and the hardening of DLC film by Ar ion implantation.

Next, a study was conducted on the various properties of DLC film when the bias voltage is fixed at -100V and the hydrogen content is changed. The hydrogen content was adjusted by changing the flow ratio of Ar and CH<sub>4</sub> gas during deposition. Fig. 6 shows the change in hardness, measured by a nano-indenter, with the hydrogen content, measured by ERDA, in DLC films. The maximum hardness is reached when the hydrogen content is

approximately 10 at% and decreases linearly with higher hydrogen content.

Furthermore, a study was conducted on the correlation between the film hardness and the structure of DLC films. A DLC film has an amorphous structure, not having any crystal structure. Therefore, the techniques, such as X-ray diffraction (XRD), commonly used for the structure analysis of metallic materials cannot be applied. Hence, the Raman spectrometry is generally used as

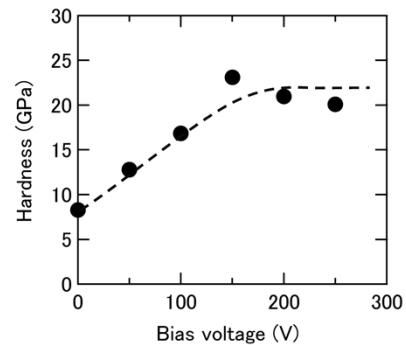


Fig. 4 Relationship between DLC film hardness and bias voltage<sup>8)</sup>

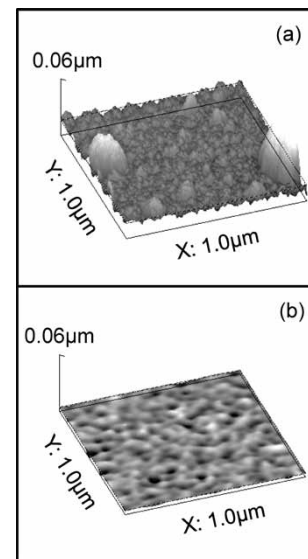


Fig. 5 AFM images of DLC film surface with negative bias voltage (a) 0V, (b) 200V<sup>8)</sup>

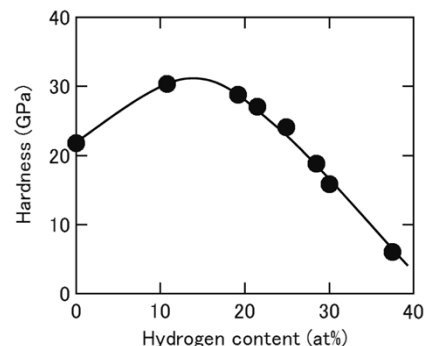


Fig. 6 Relationship between DLC film hardness and hydrogen content<sup>8)</sup>

a convenient non-destructive technique for structure analysis. This technique includes irradiating a specimen with light of a specific wavelength and estimating the bonding state, etc., of atoms using the amount of the change in the wavelength of scattered light obtained. In the case of DLC films, the structure can be estimated from the intensity ratio and positions of the G-peak (near  $1,560\text{cm}^{-1}$ ) derived from the graphite constituent and D-peak (near  $1,360\text{cm}^{-1}$ ) showing the disorder of  $\text{sp}^2$  bonding. Fig. 7 shows a Raman spectrometry result for specimens prepared for the test shown in Fig. 6. Each specimen has a G-peak shaped with a gentle shoulder at the D-peak position and shows the peak shape of a typical DLC film. Peak fitting was carried out on the basis of Fig. 7 to determine the strength ratio of the D-peak/G-peak and the position of the G-peak. No difference was found in the values for each specimen. The results of the Raman spectrometry exhibited no correlation between the structure and hardness.

Next, the density of the DLC film was determined from the RBS measurement. Fig. 8 shows the correlation between the hydrogen content and film density in a DLC film. Fig. 8 shows the same tendency as the relationship between hardness and hydrogen content shown in Fig. 6, suggesting that the hardness of the DLC film deposited by the UBMS process depends on the density of the DLC film.

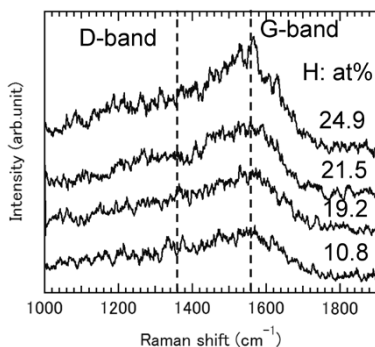


Fig. 7 Raman spectrum of DLC films with various hydrogen content<sup>8)</sup>

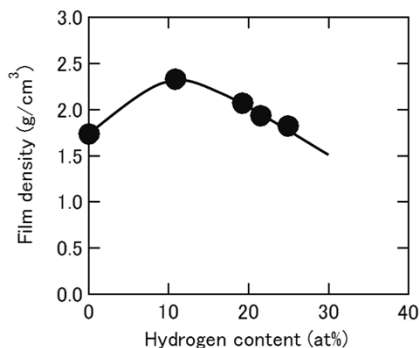


Fig. 8 Relationship between film density and hydrogen content in DLC film<sup>8)</sup>

## 2.2 Evaluation of sliding properties in oil

When DLC films are used in lubricating oil, the sliding properties change greatly not only in accordance with the properties of the DLC films but also by the types of agents added to the lubricating oil. A study was conducted on the combination of DLC film properties and additive agent in lubricating oil from the viewpoint of friction coefficient and wear volume. For the sliding test, the test apparatus described in Section 1.2 (Fig. 3) was used.

Fig. 9 compares the results of friction tests at the lowest speed ( $0.02\text{ m/s}$ ). The tests were conducted in four types of lubricants, i.e., base oil (PAO), PAO + GMO (3 wt%), PAO + phosphite (3 wt%), and PAO + amine phosphate (3 wt%); the relationships between the average friction coefficient and hydrogen content in the DLC film are shown. The results indicate that the base oil (PAO) exhibits a friction coefficient below 0.1 for a hydrogen content of about 10 at% or less, and the friction coefficient tends to increase with increasing hydrogen content. On the other hand, in the case of base oil with an additive agent, the friction coefficient is lower than that of base oil alone, and a reduction of the friction coefficient is observed even when the hydrogen content is in the range of 10 to 30 at%. In the case of GMO addition, it has been known that the friction coefficient is reduced by combination with hydrogen-free DLC film.<sup>1)</sup> The present study has shown that the same effect is at work in the film containing hydrogen. The phosphite added lubricant reduced the friction coefficient of DLC film containing as much as approximately 30 at% of hydrogen. Compared with other additive agents, the phosphite addition is shown to be effective for DLC films containing a larger amount of hydrogen.

Fig.10 shows the wear volume of a DLC film and vanes after a sliding test in which a disk (DLC film) containing 26 at% of hydrogen was used. The

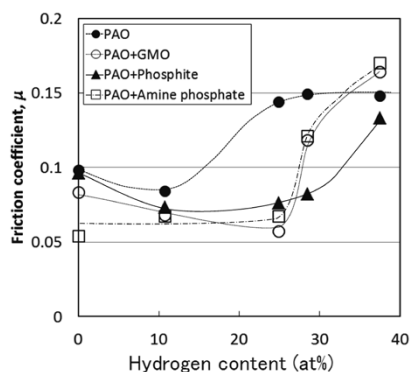


Fig. 9 Relationship between friction coefficients and hydrogen content in DLC films

wear volume of the DLC film decreases with the introduction of additive agent, and the phosphoric acid system has a greater decreasing effect on wear volume than does GMO. Regarding the wear volume of the vanes, the addition of phosphite or amine phosphate exhibits the same level of effect as the base oil without any additive agent. However, the addition of GMO results in an increase, compared with the base oil alone.

Fig.11 shows the optical micrographs of sliding portions of the DLC films and vanes shown in Fig.10. Wear scars were observed on the DLC film surfaces except for the one tested with phosphite addition. In the observation of the wear scars on the vanes, the base oil resulted in the formation of accretion on the sliding portion, whereas the phosphite addition resulted in a slight accretion on the sliding portion and accretion on the non-sliding portion as well. Furthermore, in the cases of GMO addition and amine phosphate addition, no clear accretion was observed in the sliding portion, while accretion was observed in the non-sliding portion.

For the discussion of accretion and the behavior of friction wear, TEM observation was made on

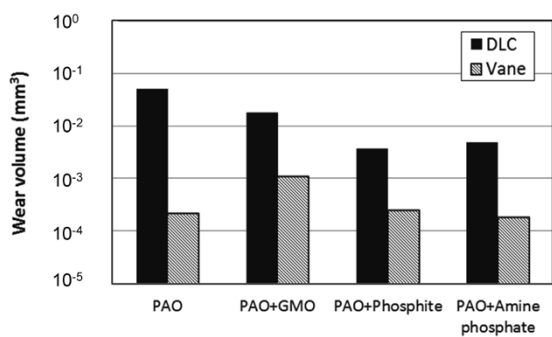


Fig.10 Wear volume of DLC disk and SUJ2 vane after sliding tests

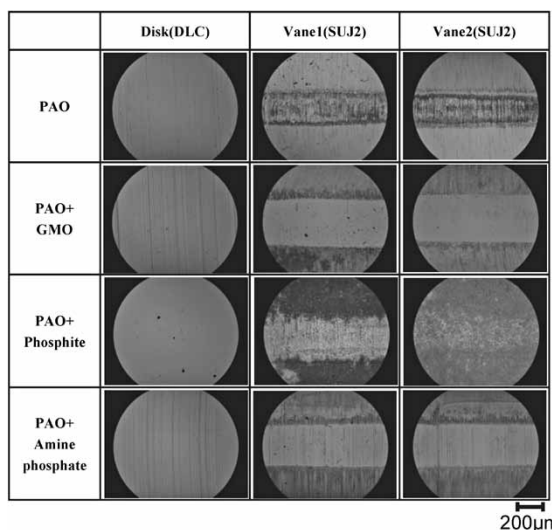


Fig.11 Optical microscope images of DLC disk and SUJ2 vane after sliding tests

the cross-section of the sliding portions of the DLC films and vanes. Fig.12 shows the cross-sectional TEM image of the sliding portion of the DLC film after the sliding test with the addition of amine phosphate shown in Fig.11. The figure on the left (a) is a full image, and the one on the right (b) is an enlargement of the vicinity of the outermost surface (sliding portion). No clear reaction product was confirmed on the DLC film surface after the sliding test, and only the amorphous structure of the DLC film was confirmed from the diffraction pattern of the enlarged image (figure on right (b)). Also, the composition analysis by AES shows predominantly carbon constituent derived from the DLC. The same result was obtained for other DLC film surfaces after the test, and no definite reaction product was formed on any sliding surface of the DLC films.

On the other hand, it was confirmed that accretion was formed on all the specimens, as shown in the cross-sectional TEM images of vane surface after the sliding test as shown in Fig.13. These accretions are considered to be tribofilms (reaction films composed of DLC film, vane (SUJ 2) and oil derived constituent, formed on the sliding surfaces during sliding). The formation of these tribofilms is considered to have greatly affected the friction wear behavior. Table 1 summarizes the results of the sliding test, TEM observation of Fig.13 and the composition analysis of the tribofilms by AES. In the

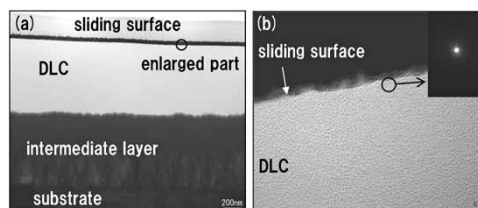


Fig.12 Cross-sectional TEM images of DLC surface after sliding test in amine phosphate additive oil

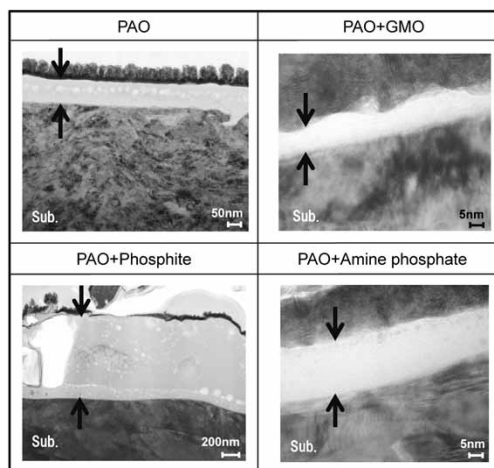


Fig.13 Cross-sectional TEM images of vane surface after sliding tests

**Table 1** Results of sliding tests in various types of lubricating oil

	Hydrogen content ( $\mu < 0.1$ )	Disk wear	Vane wear	Content of tribofilm	Tribofilm thickness
PAO	< 11at%	1	1	Fe-C-O	about 100 nm
PAO+GMO	< 25at%	0.36	5.15	Fe-C-O	about 10 nm
PAO+Phosphite	< 29at%	0.07	1.16	Fe-P-O	over 1 $\mu$ m
PAO+Amine phosphate	< 25at%	0.10	0.86	Fe-P-C-O	about 20 nm

cases of the base oil and GMO addition, tribofilms based on Fe-C-O are formed on the surfaces of the vanes. When the base oil is used as is, a thick tribofilm based on Fe-C-O is formed. It is inferred that the friction coefficient became high due to the high shear resistance of this tribofilm.

On the other hand, another tribofilm, also based on Fe-C-O but having a low shear resistance, is considered to have formed when GMO is added. In the case of GMO addition, however, the wear volume of the vane is larger, and the tribofilm is as thin as about 10 nm. Thus, it is inferred that a less protective film is formed on the vane, and the wearing vane continued to supply the tribofilm based on Fe-C-O.

In the case of phosphite addition, a tribofilm based on Fe-C-O was formed as thick as 1  $\mu$  m or more. This film seems to have enabled both the reduced wear volume of vanes and reduced shear resistance (low friction).

Furthermore, in the case of amine phosphate addition, a film based on Fe-P-C-O with reduced shear resistance is considered to have formed. It should be noted, however, that despite the formation of a tribofilm as thin as approximately 20 nm, amine phosphate can achieve both the reduction of vane wear volume and low friction. The phosphorus based constituent seems to have caused behavior different from that of GMO.

Although in the same phosphorus system, phosphite and amine phosphate are different in the presence of amine constituent, and the amine constituent included in amine phosphate seems to have contributed to the friction wear behavior. Hence, in order to investigate the influence of the amine constituent, time-of-flight secondary ion mass spectrometry (TOF-SIMS) apparatus was used to analyze in more detail the sliding and non-sliding portions of the DLC film surface after the sliding test in the oil containing amine phosphate, the details of which could not be confirmed by the cross-sectional TEM observation. Thus, the phosphate constituent has been confirmed as concentrating in the sliding portion of the DLC film, and the C-N based

constituent derived from amine was confirmed as occurring in the entire DLC film surface irrespective of its location in the sliding portion or the non-sliding portion. From this, it is inferred that the phosphate constituent concentrating on the sliding portion improves the wear resistance and that the CN constituent present in the entire DLC film surface contributes to the reduction of the friction coefficient. The TOF-SIMS observes and analyzes the molecular bonding states at adsorption levels and captures microscopic phenomena finer than the tribofilm on the vane surfaces observed by cross sectional TEM. The correlation between the formation of tribofilm and adsorption, as well as the detailed effect of each additive agent, will be future subjects.

From the above results, it was found that both a low friction coefficient and wear resistance can be achieved at the same time by using a DLC film with controlled hydrogen content in combination with an appropriate additive agent.

## Conclusions

The UBMS apparatus can change the hydrogen content and mechanical properties in DLC films by controlling the deposition conditions. Assuming parts for automobile engines, sliding tests were performed in lubricating oil. It has been clarified that low friction and low wear can both be achieved by appropriately combining the control of hydrogen content and the additive agent in lubricating oil. The application of this technology to sliding parts of automobile engines is expected to reduce friction loss and contribute to the improvement of fuel consumption.

## References

- 1) A. Erdemir et al. *Superlubricity*. ELSEVIER, 2007, pp.471-492.
- 2) T. Higuchi et al. Proceedings of the Society of Automotive Engineers of Japan. 2011, No.154-11, pp.13-16.
- 3) Y. Murakami et al. *The Tribology*. 2010, No.272, pp.44-47.
- 4) H. Tachikawa et al. *Materia Japan*. 2005, Vol.44, No.3, pp.245-247.
- 5) J. Robertson. *Mater. Sci. Eng. R. Rep.* 2002, Vol.37, pp.129-281.
- 6) K. Bewilogua et al. *Thin Solid Films*. 2004, Vol.447-448, pp.142-147.
- 7) C. Donnet et al. *Tribology of Diamond-Like Carbon Films*. Springer, 2008, pp.339-361.
- 8) H. Ito. The Japan Society of Plasma Science and Nuclear Fusion Research. 2016, Vol.92, No.6, pp.454-459.
- 9) K. Akari. R&D Kobe Steel Engineering Report. 2008, Vol.58, No.2, pp.28-31.
- 10) Denso Co. Ltd. et al. *DIAMONDLIKE CARBON HARD MULTILAYER FILM FORMED BODY, AND PRODUCTION METHOD THEREFOR*. JP2003171758, 2003-6-20.
- 11) T. Sawa et al. *J. Mater. Res.* 2001, Vol.16, pp.3084-3096.